High resolution isotropic diffusion imaging in post-mortem neonates: a feasibility study

Amy R McDowell, PhD[1], Susan C Shelmerdine[2], David W Carmichael, PhD[1,3], Owen J Arthurs, PhD[2]

[1]UCL Great Ormond Street Institute of Child Health, London, UK

[2]Department of Radiology, Great Ormond Street Hospital for Children NHS Foundation Trust, London, WC1N 3JH, UK

[3]Wellcome EPSRC Centre for Medical Engineering, King's College London, St Thomas' Hospital, London SE1 7EH

Address correspondence to:

*Dr Amy McDowell, Developmental Imaging and Biophysics, UCL GOS Institute of Child Health, 30 Guilford St, London, WC1N 1EH, UK

E mail: a.mcdowell@ucl.ac.uk; Tel 0207 905 2192; Orchid No. 0000-0002-4886-6191

Type of manuscript: Short communication

Running Title: PM neonatal HR isotropic diff imaging

Word count: 2499

Key words: Autopsy, postmortem, MRI, diffusion, paediatric, perinatal

Disclosures

There are no known conflicts of interest to disclose

Ethics

Ethical approval for the study is detailed in the Methods section.

Authorship

All authors have made substantial contributions to 1) substantial contributions to conception and design, or acquisition of data, or analysis and interpretation of data; 2) drafting the article or revising it critically for important intellectual content; and 3) final approval of the version to be published.

Abstract

Objectives

To investigate the potential of advanced diffusion imaging in Post-Mortem MRI (PMMR) at 3T.

Methods

We acquired PMMR brain and body imaging in 12 neonates, mean gestational age 33.4 weeks (range 29-37 weeks) at 3T and 1.5T. Head and body diffusion imaging at 1.5T using bipolar diffusion encoding and single-shot echo-planar imaging (EPI) for acquisition (TE 96ms; TR 2700ms; voxel size 1.8x1.8mm in-plane with slice thickness 5mm; b values of 500 and 1000 s/mm^2 applied in three orthogonal directions; total acquisition time 2:12). A whole-body 3T diffusion imaging protocol using monopolar diffusion encoding and simultaneous multi-slice EPI acquisition with gradients applied in 12 uniformly distributed directions were obtained (TE 53.4ms; TR 5600ms; 1.8mm isotropic; multi-band factor 2; b-values of 250, 750, 1250 and 1750 s/mm^2; acquisition time 2:09 for a single b-value,).

Results

There was significant improvement in image quality in multiband, multi-slice diffusion PMMR protocol. On visual assessment of image quality, 1.5T DWI scored poorly (mean 2.4 SD ± 0.47), and all 3T b values individually scored significantly higher (p<0.001) apart from b=250 which was not significantly different.

Conclusion

Recent advances in diffusion sequences and hardware utilising higher field strengths and gradient performance allows whole-body diffusion PMMR imaging at high resolution with improved image quality compared to the current clinical approach.

Advances in knowledge

We have demonstrated feasibility of a multi-slice, multi-band quantitative diffusion imaging sequence in the perinatal post-mortem setting. This will allow more detailed and quantitative clinical PMMR investigations using diffusion MRI in the future.

1

Introduction

Post mortem imaging is rapidly developing into a useful autopsy tool in the assessment of fetal and perinatal death(1), both for clinical diagnosis and exclusion of major congenital abnormalities(2). A wide range of processes following death cause alterations in water movement between and within cells and can involve cell swelling, membrane changes and breakdown. Diffusion MRI is a non-invasive method that is exquisitely sensitive to water diffusion. Advanced diffusion image acquisition and processing aims to probe the cellular diffusion environment and may throw light on different processes occurring within the tissue(3-5), which in turn has the potential to be predictive of clinical factors relating to time from and cause of death(6-8).

Post mortem MRI (PMMR) has generally adopted conventional MR sequences used in live neonatal imaging, where patient movement necessitates rapid acquisition of relatively low resolution images. In the latest review of PMMR imaging sequences(8), few centres include diffusion imaging in their clinical imaging protocols, and those that do will acquire separate axial brain and body non-isotropic diffusion imaging at few b-values, typically at 1.5T(9). This approach yields a low spatial resolution dataset, with poor characterisation of the diffusion signal (in terms of diffusion b-values and angular resolution), from which reliable data on cellular behaviour may be difficult to infer.

The simultaneous multi-slice (SMS) pulse sequence applies a multiband or composite RF pulse with a slice-selective gradient to simultaneously excite multiple slice planes within the imaging volume. This increases acquisition efficiency by exciting several slices simultaneously, leading to higher resolution images in the same acquisition time and/or shorter acquisition times (10). In standard 2D k-space encoding, the signal from simultaneously excited slices are mixed together, but they can be separated using the spatial encoding information inherent in a multi-coil receiver system as used in modern imaging. SMS sequences are available across field strengths, but the measurement of diffusion indices is likely to be improved by higher performing gradients, optimised B_0 shimming, and multi-channel RF coil technology, as well as the higher signal at higher field strengths, which are often more prevalent in more modern 3T scanners. A combination of

2

this multi-slice approach and one of the reduced phase-encode techniques such as sensitivity encoding (SENSE) further increases efficiency(11). It should be noted that post-mortem work on a clinical scanner is still subject to specific absorption rate (SAR) limitations even though these are no longer relevant. These impose restrictions on the sequence, as the composite RF pulses using in SMS sequences are prone to exceed peak amplitude capabilities of the RF amplifier and the total power in the pulse may exceed these SAR limits. Methods can be employed to reduce peak amplitude without affecting SAR or that achieve time-averaged power reduction(12), to improve this.

In this article, our aim is to investigate the potential of using advanced diffusion sequences recent MRI hardware improvements for perinatal PMMR autopsy over conventional diffusion imaging. In this feasibility study, the use of multiband sequences should allow faster acquisition by obtaining two or more slices with increasing acceleration factor (at the same time as one slice)(13-15). Coupled with improved gradient performance (that allows for high quality monopolar diffusion encoding at short echo times), this enables acquisition of increased resolution, isotropic images of the whole body, and a better characterisation of the diffusion signal, increasing resolution in the diffusion domain, by allowing for diffusion weighted images at a range of b-values and gradient directions in the equivalent time to current practice derived from neonatal clinical imaging. As there is no patient movement during the PMMR, a single isotropic resolution volume combining both the head and body can be acquired, allowing full visualisation in all planes. We evaluated the feasibility of this approach through visual assessment of image quality and quantification of MD values to provide a comparison to current clinical practice.

Methods

We prospectively acquired post-mortem magnetic resonance imaging from cases referred to our institution for perinatal autopsy. Written informed consent was obtained for all patients for clinical pre-autopsy PMMR as part of our institution's clinical post mortem assessment. Bodies were stored in a mortuary at 4°C and PMMR was performed outside of normal working hours to ensure as little disturbance as possible to clinical services. Cases were brought directly from the mortuary and positioned in a head coil in the supine position, and wrapped in insulating material to aid temperature stability.

Conventional 1.5T diffusion PM MR Imaging

Clinical imaging was performed at 1.5 T Avanto scanner (Siemens Medical Solutions, Erlangen, Germany) including post-mortem brain and body imaging with standard 3D T1-weighted and T2-weighted sequences according to previously published protocols(8). Conventional Diffusion weighted imaging was performed using single-shot spin-echo echo-planar imaging (SE-EPI), utilising a twice-refocused sequence(16) to improve eddy current performance. Imaging parameters are given in Table 1. From the native diffusion acquisition, apparent diffusion coefficient (ADC) maps were obtained on the acquisition console (Syngo, Siemens Medical Solutions, Erlangen, Germany).

3T Multiband Diffusion Imaging

Whole body (vertex to mid-thigh) images were performed with a 3T Siemens Prisma The multi-shell diffusion sequence employed a diffusion-weighted spin-echo single shot 2D EPI acquisition, with multi-band radio frequency pulses to accelerate volume coverage along the slice direction. A single refocused SE-EPI diffusion sequence was used to enable the TE to be shortened reducing T2 decay and increasing signal levels while reducing the TR and giving a faster scan time. Image distortion due to tissue magnetic susceptibility-related B0 field perturbations is increased at 3T and were compensated for by acquiring a short reversed phase encoding scan for correction with no diffusion encoding and all other EPI parameters being the same. Imaging parameters are given in Table 1. The acquired data was corrected for distortion using TopUp (https://fsl.fmrib.ox.ac.uk/fsl/fslwiki/topup) within TractoR (http://www.tractor-mri.org.uk). Mean diffusivity (MD) tensor maps were

4

generated using FSL version 5.0.9 using all 12 directions and a weighted least squares regression fit.

<u>Image Interpretation</u>

Regions of Interest (ROIs) were drawn manually using MIPAV and plotted on the MD maps by a single operator, a Radiology Fellow with 7 years radiology training, saved as a VOI dataset and overlaid across all sequences. The regions of interest were placed in Frontal Lobe white matter (WM), Frontal Lobe grey matter (GM), Temporal Lobe WM, Temporal Lobe GM, Occipital Lobe WM, Occipital Lobe GM, Basal Ganglia, Pons, Cerebellum, Right Lung, Left Lung, Myocardium, Right Lobe Liver, Left lobe liver, Spleen, Right Renal Cortex, Left renal cortex, Right Psoas and Left Psoas (as described in previous publications (7, 17)). MD maps derived from both combined and single b-value images (acquired at 3T only) were also blindly scored for image quality / diagnostic acceptability by the same operator using a simple visual analogue scale:

    1 = unacceptable, no diagnosis possible;

    2 = marked artefacts, no diagnosis possible;

    3 = acceptable, diagnosis possible;

    4 = very good, diagnosis possible;

    5 = excellent, diagnosis possible;

T-tests were performed between 1.5T scores versus all b-values and combined b-values at 3T, and all combined b-values scores versus all other b-values at 3T and 1.5T.

<u>Temperature measurement</u>

Temperature was measured using an electronic thermometer in the same anatomical position (armpit or groin) immediately before transfer into the MR scanner, this is typically 1-2 minutes before the first scan and a 1-2 minutes after removal of the neonate from the scanner, the position of thermometer was replicated for both time points. Temperature values in each neonate were estimated by assuming a linear gradient temperature change across the imaging session, and the temperature was taken at the mid time point of the diffusion scan. Subjects were viewed in all three orthogonal planes in the MD scan at the centre time point, and a ROI drawn in the in the large lobe of the liver for homogeneity. The

5

average values of these ROIs were then plotted against time to examine any correlation of MD with time.

Results

12 neonates underwent PM MR imaging with gestational age 33.4 ± 3.3 weeks (range 29-37 weeks). 11 cases were stillbirths or intrauterine deaths, from which no cause of death in the fetus was found (most causes of death related to placental insufficiency, placental infection or no cause found); one case was a termination of pregnancy for suspected CNS abnormality which was normal at imaging and autopsy.

The mean temperature across subjects at scan time was found to be 8°C (range 6.2 – 11.2 °C). The correlation coefficient R^2 between temperature at time of scan and MD in the liver of each neonate was found to be 0.35 with a P-value of 0.09. We did not correct our MD values for temperature because this correlation was not significant and the effects of this temperature range on MD were reasonably small compared to other sources of variance affecting the MD in our sample.

On visual assessment of image quality, 1.5T DWI scored poorly (mean 2.4 SD ± 0.47), and all 3T b-values individually scored significantly higher (p<0.001) apart from b=250 which was not significantly different (Figure 1). Single b-value MD maps at higher b-values contained more detail (Figure 2), and there was an increase in diagnostic acceptability with higher b-values. The highest score were for the combined b-value 3T dataset (Figure 1), but there was little difference between this and the highest single b-value of 1750 s/mm^2. This demonstrates that a higher b-values are optimal in post-mortem imaging. T-test results are shown in Figure 2.

Average MD values were obtained from all organs in all cases and shown in Figures 3 respectively. Brain and solid organ MD values are comparable to those obtained in previous studies (6, 7). Myocardium and psoas muscle were found to have the highest MD values (Figure 3).

7

Discussion

We have demonstrated feasibility of using a multiband diffusion imaging sequence in the perinatal post mortem setting. This sequence allowed the acquisition of higher (isotropic) resolution images of whole body with higher image quality, in the equivalent time to typical imaging adapted from neonatal clinical imaging. The ability to obtain detailed quantitative MD values may give diagnostic benefit for perinatal postmortem imaging assessment.

Isotropic diffusion imaging at this level of resolution and field strength has not been performed before in neonatal PMMR imaging. Previously published clinical post-mortem diffusion work typically had low resolution in the slice direction; Schmidt et al(18) measured ADC values in the adult post-mortem brain, acquiring standard 5mm slices at 1.5T in the tranverse (axial) orientation. Haakma et al(19) performed tractography in adult post-mortem subjects at 1.5T, with 3 mm isotropic voxel resolution. Diffusion images with b-values of 0 and 2000 s/mm^3 and 15 directions were acquired of the lumbar and sacral nerves. All three previous publications on perinatal post mortem diffusion imaging are from our institutions, and all three investigated diffusion imaging at 1.5T with a slice thickness of 5mm with gradient values of 0, 500, 1000 s/mm^3(6, 7, 20). We also note that other published work often quotes ADC values, although it is frequently unclear whether a single direction or the average of three directions was measured. We have chosen to use Mean Diffusivity which is defined as the average of the three eigenvalues of the tensor, or the magnitude of diffusion regardless of direction, to avoid any ambiguity.

The multiband diffusion imaging sequence at 3T gave superior imaging quality due to a combination of increased signal at higher field strength, an increase in speed of acquisition due to the multiband sequence, the gradient performance which provides both shorter diffusion encoding times directly and because improved eddy current performance enables single refocused diffusion encoding to be used with acceptable image quality. Together this enables the use of much shorter TEs, therefore increasing SNR due to a reduction in T$_2$ decay whilst also reducing scan time per slice. Taken together with the use of a higher field strength, a higher resolution scan can be acquired in the same overall scan time. Acquiring one isotropic acquisition of the whole body provides easy visualisation which can be viewed in all three orthogonal planes at increased resolution, allowing quantitation of diffusion

8

indices in the smaller neonatal organs. However, the real benefit of this scan protocol is that it provides a fuller characterisation of changes in the diffusion signal (owing to the range of b-values and gradient directions used) that can be used to try to infer underlying processes that occur during and after death in addition to being used for standard clinical practise. Therefore the feasibility of obtaining this information in a single short scan with whole body coverage provides a useful starting point for research in this area. A larger future study will be required to evaluate the performance of this sequence against histological validation, and in specific clinical scenarios.

The acquisition of high resolution whole body imaging has significant clinical advantages over conventional sequences, with improved resolution at higher b-values. Recent studies confirm that higher resolution post mortem imaging at 3T improves overall clinical diagnostic accuracy compared to 1.5T (9). The average mean diffusivity values in the grey matter of the brain are higher than the white matter as expected. The myocardium and psoas muscles shows a high value of mean diffusivity, which may be due to an underlying change in cell wall permeability. While b-values could be further optimised in different organs, obtaining a range of b-values within the whole body is a simpler approach at the early evaluation stage, and the whole dataset can be used for more complex models of diffusion.

A limitation of our study is that like all feasibility studies in a small cohort of late gestation fetuses, the results may not be generalisable to other study populations such as very early gestational fetuses (15-20 weeks). Nevertheless, in this feasibility study, the quality of the images and the values MD obtained offer a clear advantage over those in the existing literature. The application of the technique in a larger cohort of perinatal deaths across different gestational ages are required to characterise diagnostic performance. However, the approach of taking a range of b-values (made possible by the high SNR and efficiency of the sequence) means that the data is appropriate for a very wide range of tissue properties and so is likely to be appropriate in a bigger cohort. Of particular interest will be the comparison of the results of diffusion parameters with histological organ sampling where available, as the wide range of MD values in this cohort may correspond to underlying histological variation.

9

Conclusion

We have demonstrated feasibility of a multi-slice multiband quantitative diffusion imaging sequence in the perinatal post mortem setting. The rapid acquisition of high resolution whole body imaging may have significant clinical advantages over conventional sequences, reducing partial volume effects. In addition, it allows a fuller characterisation of the diffusion signal by allowing diffusion images with a range of b-values and gradient directions to be obtained which may allow tissue changes post-mortem to be better characterised, and opens up the possibility of obtaining more specific measures of tissue microstructure. We predict that this will become a useful additional tool in evaluation perinatal death in a clinical setting.

References

1.   Nicholl RM, Balasubramaniam VP, Urquhart DS, Sellathurai N, Rutherford MA. Postmortem brain MRI with selective tissue biopsy as an adjunct to autopsy following neonatal encephalopathy. European journal of paediatric neurology : EJPN : official journal of the European Paediatric Neurology Society. 2007;11(3):167-74.

2.   Arthurs OJ, Taylor AM, Sebire NJ. Indications, advantages and limitations of perinatal postmortem imaging in clinical practice. Pediatric radiology. 2015;45(4):491-500.

3.   Ding AY, Li Q, Zhou IY, Ma SJ, Tong G, McAlonan GM, et al. MR Diffusion Tensor Imaging Detects Rapid Microstructural Changes in Amygdala and Hippocampus Following Fear Conditioning in Mice. PLoS ONE. 2013;8(1).

4.   Nilsson M, van Westen D, Stahlberg F, Sundgren PC, Latt J. The role of tissue microstructure and water exchange in biophysical modelling of diffusion in white matter. Magma (New York, NY). 2013;26(4):345-70.

5.   Froeling M, Oudeman J, Strijkers GJ, Maas M, Drost MR, Nicolay K, et al. Muscle changes detected with diffusion-tensor imaging after long-distance running. Radiology. 2015;274(2):548-62.

6.   Papadopoulou I, Langan D, Sebire NJ, Jacques TS, Arthurs OJ. Diffusion-weighted post-mortem magnetic resonance imaging of the human fetal brain in situ. European journal of radiology. 2016;85(6):1167-73.

7.   Arthurs OJ, Price GC, Carmichael DW, Jones R, Norman W, Taylor AM, et al. Diffusion-weighted perinatal postmortem magnetic resonance imaging as a marker of postmortem interval. European radiology. 2015;25(5):1399-406.

8.   Norman W, Jawad N, Jones R, Taylor AM, Arthurs OJ. Perinatal and paediatric post-mortem magnetic resonance imaging (PMMR): sequences and technique. The British journal of radiology. 2016;89(1062):20151028.

9.   Kang X, Cannie MM, Arthurs OJ, Segers V, Fourneau C, Bevilacqua E, et al. Post-mortem whole-body magnetic resonance imaging of human fetuses: a comparison of 3-T vs. 1.5-T MR imaging with classical autopsy. European radiology. 2017;27(8):3542-3553.

10.   Feinberg DA, Setsompop K. Ultra-fast MRI of the human brain with simultaneous multi-slice imaging. Journal of Magnetic Resonance. 2013;229:90-100.

11.   Larkman DJ, Hajnal JV, Herlihy AH, Coutts GA, Young IR, Ehnholm G. Use of multicoil arrays for separation of signal from multiple slices simultaneously excited. Journal of magnetic resonance imaging : JMRI. 2001;13(2):313-7.

12.   Barth M, Breuer F, Koopmans PJ, Norris DG, Poser BA. Simultaneous multislice (SMS) imaging techniques. Magnetic resonance in medicine. 2016;75(1):63-81.

13.   Feinberg DA, Moeller S, Smith SM, Auerbach E, Ramanna S, Gunther M, et al. Multiplexed echo planar imaging for sub-second whole brain FMRI and fast diffusion imaging. PLoS One. 2010;5(12):e15710.

14.   Setsompop K, Cohen-Adad J, Gagoski BA, Raij T, Yendiki A, Keil B, et al. Improving diffusion MRI using simultaneous multi-slice echo planar imaging. NeuroImage. 2012;63(1):569-80.

15.   Setsompop K, Gagoski BA, Polimeni JR, Witzel T, Wedeen VJ, Wald LL. Blipped-controlled aliasing in parallel imaging for simultaneous multislice echo planar imaging with reduced g-factor penalty. Magnetic resonance in medicine. 2012;67(5):1210-24.

11

16.   Reese TG, Heid O Fau - Weisskoff RM, Weisskoff Rm Fau - Wedeen VJ, Wedeen VJ. Reduction of eddy-current-induced distortion in diffusion MRI using a twice-refocused spin echo. 2003 Jan;49(1):177-82

17.   Arthurs OJ, Rega A, Guimiot F, Belarbi N, Rosenblatt J, Biran V, et al. Diffusion magnetic resonance imaging of the fetal brain in intrauterine growth restriction. Ultrasound in obstetrics & gynecology : the official journal of the International Society of Ultrasound in Obstetrics and Gynecology. 2017 Jul;50(1):79-87

18.   Schmidt TM, Fischer R, Acar S, Lorenzen M, Heinemann A, Wedegartner U, et al. DWI of the brain: postmortal DWI of the brain in comparison with in vivo data. Forensic science international. 2012;220(1-3):180-3.

19.   Haakma W, Pedersen M, Froeling M, Uhrenholt L, Leemans A, Boel LW. Diffusion tensor imaging of peripheral nerves in non-fixed post-mortem subjects. Forensic science international. 2016;263:139-46.

20.   Montaldo P, Chaban B, Lally PJ, Sebire NJ, Taylor AM, Thayyil S. Quantification of ante-mortem hypoxic ischemic brain injury by post-mortem cerebral magnetic resonance imaging in neonatal encephalopathy. European journal of paediatric neurology : EJPN : official journal of the European Paediatric Neurology Society. 2015;19(6):665-71.

Table legends

Table 1 *Comparison of acquisition parameters at 1.5T and 3T*

Figure legends

Figure 1 *Example MD maps of the same subject at 1.5T (left) using the standard clinical diffusion scan and a mean diffusivity map at 3T (right) using the optimised high resolution diffusion sequence with b-values of 250, 750, 1250 and 1750 s/mm^2. Example cross-sections are shown at the level of the brain, lungs and kidneys. The cross-sectional image of the brain at 3T has been re-windowed for clarity USE SLICE 21 for kidneys*

Figure 2 *Bar chart of average visual assessment scores for all neonates. Significance (p < 0.05) is shown between 1.5T scores versus all combined b-values and all other b-values at 3T*

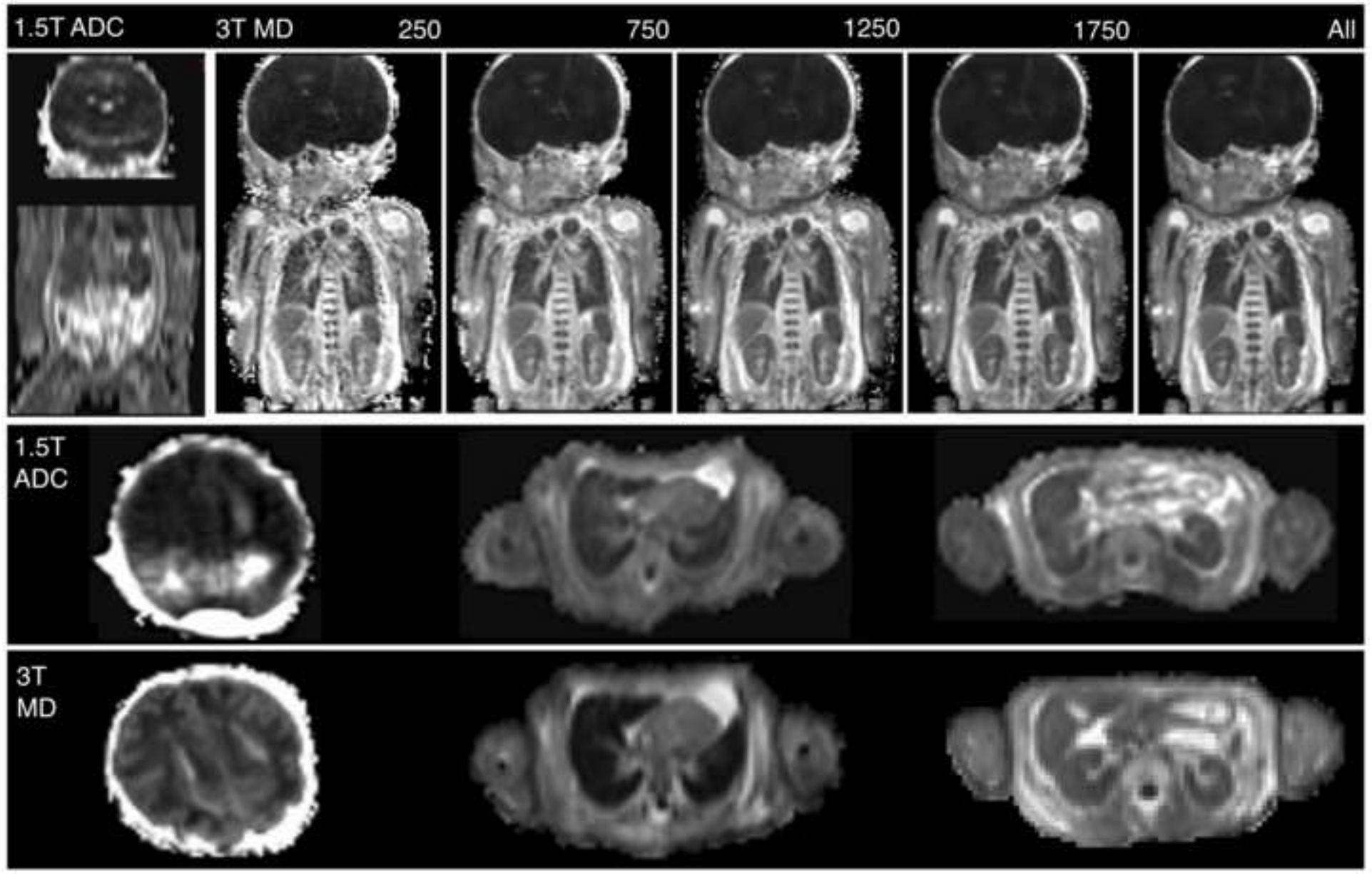*(shown by *) and all combined b-values versus all other b-values at 3T and 1.5T scores*
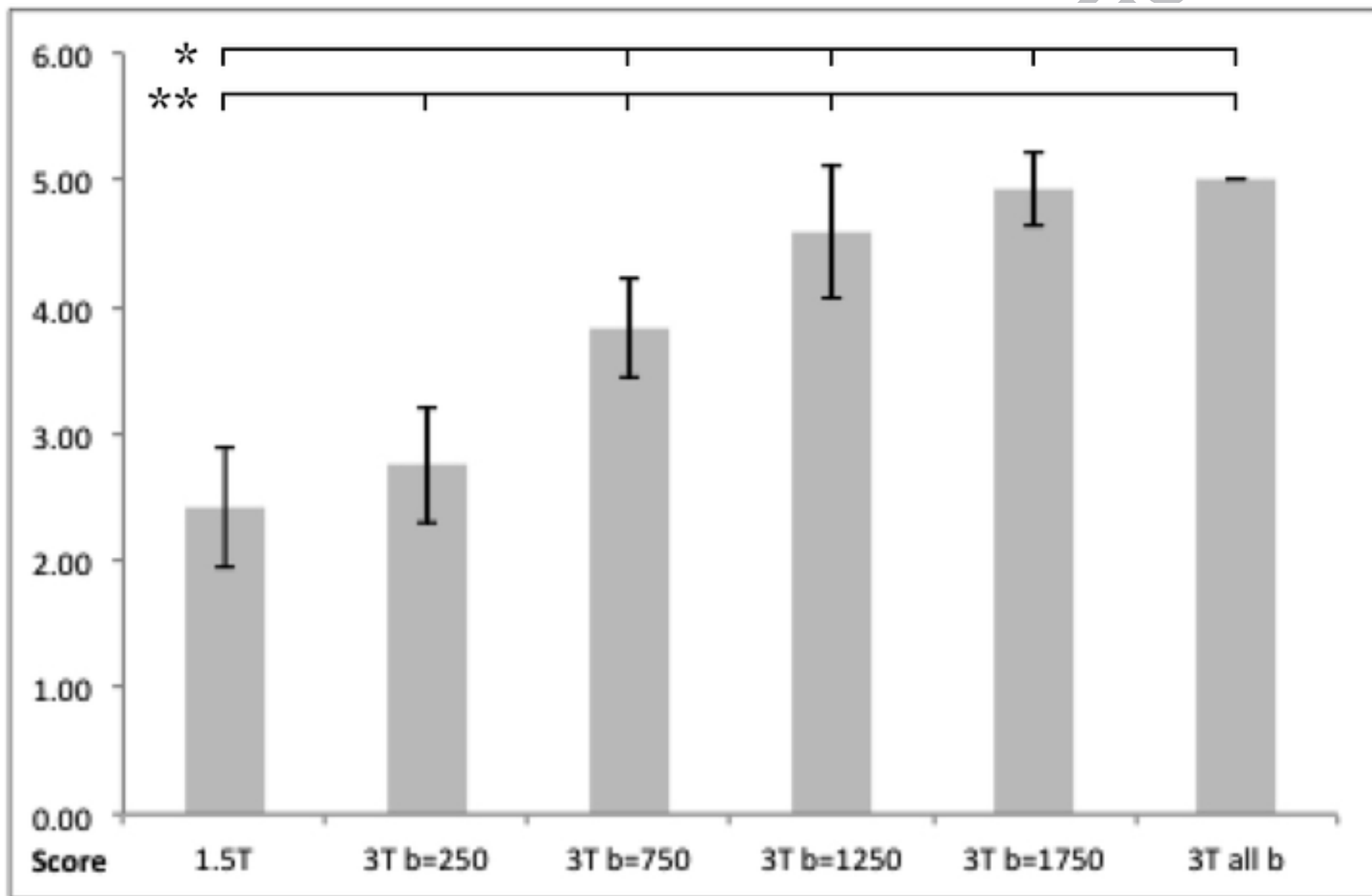
(shown by **)

Figure 3 *Average MD values in all neonates by region of interest. Values were produced using all b-values and 12 direction uniformly distributed diffusion vectors*

Table 1

Parameter	Clinical acquisition	Research acquisition in this study
Scanner type	Siemens Avanto	Siemens Prisma
Field strength	1.5 T	3 T
Gradient	40/40/45 (x/y/z) mT/m	80 mT/m
	200 T/m/s magnetic field gradients	200 T/m/s magnetic field gradients
Coil	12 channel phased-array head coil	64 channel head coil
Acquisitions	Body and brain separate acquisition	Whole body
DWI Sequences		
Sequence	Single-Shot SE-EPI (twice refocused)	2D SE-EPI (single refocused)
Plane acquisition	Axial	Axial
RF pulse type	Normal	Multiband (factor 2)
EPI factor	95	96
Voxel size	Head 5mm (5mm) Body 5mm (8.5mm)	1.8mm isotropic (1.8mm)
TR	2700 (msec)	5600 (msec)
TE	96 (msec)	53.4 (msec)
Voxel size	1.8x1.8x5.0mm	1.8mm isotropic
b-values (s/mm^2)	0, 500, 1000	0, 250, 750, 1250, 1750 (with one unweighted with reversed PE for distortion correction)
Gradient directions	3 (Orthogonal)	12 (Uniformly distributed)
Acquisition time	2 acquisitions at 1:06mins each	2:09mins for all except 1:02mins for reversed PE acquisition

14

Figure 1

Figure 2

Figure 2

Figure 3

Figure 3